Langmuir

Article

pubs.acs.org/Langmuir

Adsorption of Doxorubicin on Poly(methyl methacrylate)−Chitosan−Heparin-Coated Activated Carbon Beads

Jianjun Miao,[†,⊥,#] Fuming Zhang,[‡,⊥] Majde Takieddin,[¶] Shaker Mousa,[¶] and Robert J. Linhardt*[,†,‡,§,∥,⊥,#]

[†]Department of Chemical and Biological Engineering, [‡]Department of Chemistry and Chemical Biology, [§]Department of Biology, [∥]Department of Biomedical Engineering, [⊥]Center for Biotechnology and Interdisciplinary Studies, and [#]Rensselaer Nanotechnology Center, Rensselaer Polytechnic Institute, Troy, New York 12180, United States

[¶]Pharmaceutical Research Institute, Albany College of Pharmacy, Albany, New York 12208, United States

ABSTRACT: Extracorporeal filter cartridges, filled with an activated carbon bead (ACB) adsorbent, have been used for removal of overdosed cancer drugs from the blood. Coatings on adsorbent matrices, poly(methyl methacrylate) (PMMA)/activated carbon bead and PMMA/chitosan/heparin/ACB composites, were tested to improve their biocompatibility and blood compatibility. PMMA coating on ACBs was accomplished in a straightforward manner using a PMMA solution in ethyl acetate. A one-step hybrid coating of ACBs with PMMA−anticoagulant heparin required the use of acetone and water cosolvents. Multilayer coatings with three components, PMMA, chitosan, and heparin, involved three steps: PMMA was first coated on ACBs; chitosan was then coated on the PMMA-coated surface; and finally, heparin was covalently attached to the chitosan coating. Surface morphologies were studied by scanning electron microscopy. X-ray photoelectron spectroscopy confirmed the $-SO_3^-$ group. Adsorption, of a chemotherapy drug (doxorubicin) from both water and phosphate-buffered saline, by the coated ACBs was examined. The adsorption isotherm curves were fitted using the Freundlich model. The current adsorption system might find potential applications in the removal of high-dose regional chemotherapy drugs while maintaining high efficiency, biocompatibility, and blood compatibility.

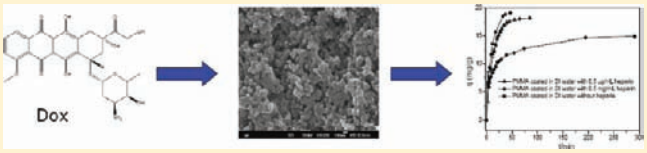

INTRODUCTION

Systemic drug delivery of potent anticancer agents exposes the entire body to toxic levels of these drugs. Localized and targeted chemotherapeutic drug delivery could potentially deliver significantly higher doses of toxic anticancer drugs, directly to a tumor where it is required, decreasing systemic toxicity and improving drug efficacy and safety. Intra-arterial chemotherapy has recently been shown to result in remarkable clinical outcomes with minimal adverse effects, as compared to systemic administration, because of higher intratumoral concentrations of oncostatics.[1−5] Increased antitumor effects are generally believed to correlate with higher dose intensity but are also associated with severe toxicity.[6] Doxorubicin (DOX) is a chemotherapy drug used in the treatment of a wide range of cancers, including liver cancer. However, DOX has significant side effects, including but not limited to severe cardiac toxicity, damage to the immune system, acute nausea, severe vomiting, dermatological problems, and hair loss. The most serious side effect of DOX, however, is irreversible heart tissue damage.[7,8] Activated carbon filter cartridges have been used to adsorb toxic drugs, removing them from the body, particularly in cases of overdose. Similarly, we envision that activated carbon filter cartridges might be used to efficiently remove the excess DOX after delivering it to a tumor site, such as the liver. This could be accomplished by isolating the liver from the systemic circulation, infusing DOX into the artery serving the liver, removing excess drug from the portal vein draining the liver using an extracorporeal filter cartridge, and returning blood free of DOX to the body. The major challenge of using such an approach is that currently available activated charcoal filters have a low first-pass adsorption capability, produce carbon debris, and activate the blood-clotting cascade, and damage blood cells. Thus, there is an urgent need for filters with high adsorption efficiency, biocompatibility, and blood compatibility.

We have previously reported that cellulose−heparin-coated charcoal is capable of adsorbing hydrophobic protein-bound drugs without causing large losses of blood proteins.[9,10] This cellulose−heparin-coated charcoal relied on a coating process using a heparin imidazolium salt dissolved in a cellulose-containing room-temperature ionic liquid and required extensive washing steps to remove the ionic liquid and convert the heparin imidazolium salt into the heparin sodium salt.

In the current study, poly(methyl methacrylate) (PMMA), a biocompatible polymer,[11] has been coated on the surface of activated carbon beads (ACBs) as a potential adsorbent for extracorporeal filter cartridges. In addition, heparin was also incorporated in these coatings to improve blood compatibility by chemical conjugation (multilayer coating containing PMMA, chitosan,[12] and heparin sodium) or physical blending (one-step hybrid coating of PMMA−heparin sodium). The heparin content, on the surface of coated ACBs, was determined by

Received: January 2, 2012
Revised: February 1, 2012
Published: February 7, 2012

dx.doi.org/10.1021/la3000137 | *Langmuir* 2012, 28, 4396−4403

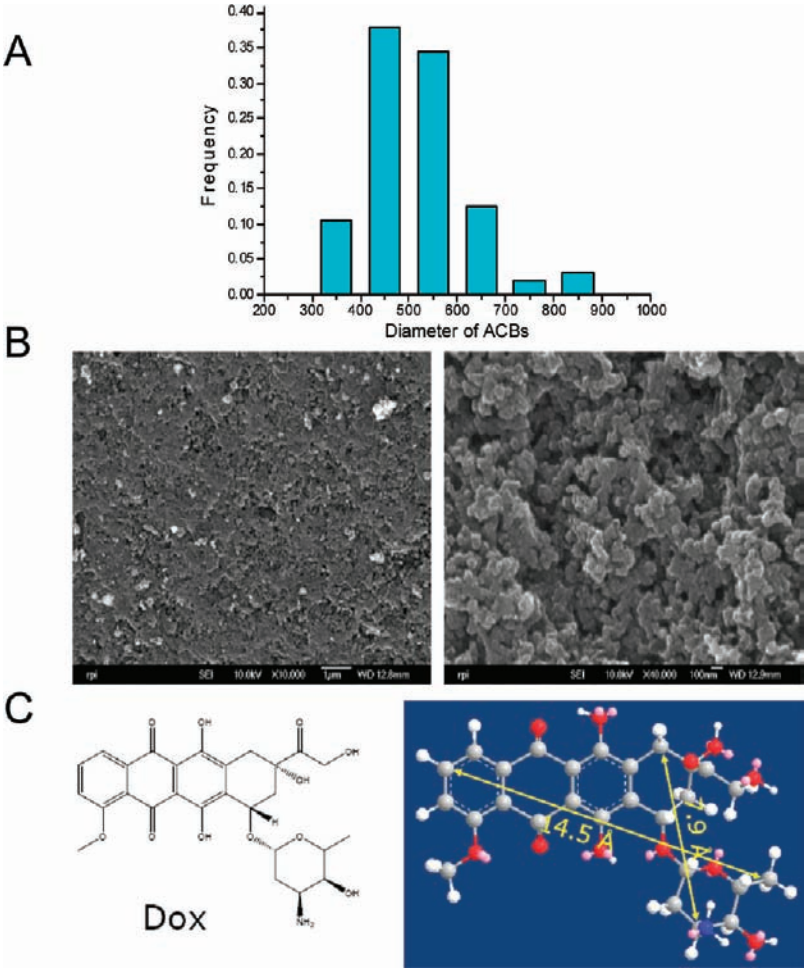

Figure 1. (A) Size distribution of uncoated ACBs based on 800 individual beads. (B) SEM images of uncoated ACBs (left image, surface; right image, cross-section). (C) Chemical structure of DOX and its molecular dimensions determined by ChemDraw 3D.

electron-dispersive X-ray spectroscopy and X-ray photoelectron spectroscopy (XPS). The chemical conjugation of heparin on the surface or ACBs also has a potential advantage that heparin does not release into the medium, which avoids the formation of heparin−DOX complexes in solution. Adsorption of DOX by coated and uncoated ACBs was tested in both water and phosphate-buffered saline (PBS; 10 mM sodium phosphate and 0.138 M sodium chloride at pH 7.4). The Freundlich model was used to study the adsorption isotherm.

MATERIALS AND METHODS

Materials. PMMA (molecular weight of 120 kDa), DOX hydrochloride, and high-molecular-weight chitosan (800 cps, Aldrich 419419)) were purchased from Sigma-Aldrich (St. Louis, MO). All solvents were obtained from Fisher Scientific (Pittsburgh, PA). Heparin sodium salt (180 units/mg) from porcine intestine was from Celsus Laboratories (Cincinnati, OH). ACBs were obtained from Dr. Vladimir G. Nikolaev of the R. E. Kavetsky Institute of Experimental Pathology, Oncology and Radiobiology NAS of Ukraine.

Characterization of ACBs. The bulk density and surface characteristics of the ACBs have been previously reported.[4] The size distribution of the current batch of spherical ACBs was determined using optical microscopy to measure the diameter of 800 individual beads. Cross-sectional morphology was observed by imaging hemispherical beads prepared by cutting ACBs with a razor blade.

Coating of ACBs with PMMA. Dry ACBs (100 g) were added into a solution of PMMA in ethyl acetate (1200 mL of 2.5%, w/v) and shaken in a 2 L beaker for 6 h at 145 rpm. After coating, the solution was decanted and the beads were dried under airflow in the hood for overnight, after which they were further dried in a vacuum oven at 80 °C.

One-Step Coating of ACBs with the PMMA−Heparin Blend Layer. Heparin sodium (50 mg) was dissolved in water (2.5 mL), and then acetone (7.5 mL) was added to obtain a clear 0.5% (w/v) solution. PMMA was prepared in acetone as 5% (w/v) for 4 mL and then was added to 4 mL of the heparin solution slowly to avoid precipitation, and the final solution was stable and off-white. Two batches of beads (1 and 2), weighing 2 and 1 g, respectively, were immersed in 16 and 8 mL of the above PMMA−heparin solution, respectively, and shaken at 180 rpm for 5 h. A total of six batches of ACBs were coated under a variety of different conditions.

Coating of ACBs with PMMA−Chitosan. Chitosan was dissolved in 0.25% (w/w) aqueous acetic acid solution at a concentration of 120 mg/16 mL. Dry PMMA-coated ACBs (1.1 g) were added to chitosan solution (8 mL), and the resulting mixture was shaken in three batches for 1, 3, and 5 h. After coating, the supernatant was decanted and the beads were filtered under vacuum through Millipore filter paper using a Bucher funnel and rinsed with 0.1 N sodium hydroxide solution and further with water to remove residual sodium hydroxide. The PMMA−chitosan-coated beads were dried overnight in a vacuum oven at 80 °C.

Immobilization of Heparin on PMMA−Chitosan-Coated ACBs. The immobilization of heparin followed the literature with slight modification.[13] Briefly, PMMA−chitosan-coated ACBs (0.3 g) were equilibrated in 2-(*N*-morpholino)ethanesulfonic acid (MES) buffer (0.05 M, pH 5.6) for 1 h. Heparin solution [5 mL of 2% (w/w) in 0.05 M MES buffer at pH 5.60] was activated by adding 1-ethyl-3-

dx.doi.org/10.1021/la3000137 | *Langmuir* 2012, 28, 4396−4403

Table 1. Physical Properties of ACBs with and without Coating by the BET Isotherm

type of ACBs	diameter (μm)	surface area (m^2/g)		pore volume (mL/g)		most frequent pore size (nm)
		no adjustment	adjustment	no adjustment	adjustment	
uncoated beads	520 ± 102	2325 ± 31	2325 ± 31	2.72 ± 0.13	2.72 ± 0.13	1.6 and 2.5–2.6
PMMA-coated beads	520 ± 101	2070 ± 26	2325 ± 29	2.37 ± 0.14	2.72 ± 0.16	1.6 and 2.5–2.6
PMMA–chitosan-coated beads	520 ± 102	1632 ± 21	2040 ± 27	1.88 ± 0.11	2.35 ± 0.14	1.8 and 2.5–2.6
PMMA–chitosan–heparin-coated beads	520 ± 102	1140 ± 15	1462 ± 19	1.47 ± 0.11	1.88 ± 0.14	1.6 and 2.5–2.6

(3-dimethylaminopropyl)carbodiimide hydrochloride (EDC) and *N*-hydoxysuccinimide (NHS) at a molar ratio of EDC/NHS/heparin of 0.4:0.24:1.0. The preactivation proceeded for 10 min, after which 0.3 g of the buffer-moistened PMMA–chitosan ACBs were added and shaken overnight at 180 rpm at room temperature. The beads were recovered by decanting and then washed for 24 h with three changes of water. The heparin-coated beads were dried overnight in a vacuum oven at 40 °C.

Adsorption Kinetics of DOX. A 110 mg portion of either PMMA-coated ACBs or PMMA–heparin one-step-coated ACBs were tested for their ability to adsorb 0.6 mg/mL DOX in a 3 mL volume of water. A 0.1 mL aliquot was removed from the adsorption vial every 3 min, added to a 2.5 mL polypropylene centrifuge tube, and brought to 0.9 mL with water. Water (0.1 mL) was added to the adsorption vial to maintain its volume. The corresponding concentrations were calculated using the appropriate dilution factor. The relative concentration was calculated as the ratio between the concentration at any given time and the initial concentration. The relative concentration was then plotted as a function of time.

In the multilayer coating, a 110 mg portion of uncoated, PMMA-coated, PMMA–chitosan-coated, and PMMA–chitosan–heparin-coated ACBs were tested using the similar procedure as used for the one-step coating. Two different solvent systems were examined, water and PBS.

Calibration Curve for DOX Solution. An ultraviolet–visible (UV–vis) calibration curve was obtained by measuring absorption maximum at 480 nm and the baseline at 600 nm for five concentrations of 0.05, 0.025, 0.0125, 0.00625, and 0.003 125 mg/mL in water. These five points were fit into a linear curve with R^2 = 0.996. Solutions of concentrations higher than 0.05 mg/mL were diluted into the range of the calibration curve to make determinations.

Adsorption Isotherm. The determination of the adsorption isotherm was carried out in 2 mL DOX solution in a 2.2 mL polypropylene centrifuge vial, with 10 mg of ACBs for each sample. The determination was performed for uncoated ACBs, PMMA-coated ACBs, and PMMA–chitosan–heparin-coated ACBs. The initial concentration was in the range between 0.0126 and 4 mg/mL in both water and PBS. The solution was shaken (220 rpm) at room temperature (22 °C) for 12 h. The adsorption capacity (q) versus the equilibrium concentration (C_e) was plotted and fitted to the Freundilich isotherm equation.

Activated Partial Thromboplastin Time (aPTT). ACBs or coated ACBs (250 mg) were gently mixed with 5 mL of human blood (citrated blood) on a rotator for 30 min. Plasma was separated by centrifugation at 1000*g* for 10 min, and aPTT was determined on an ACL8000 automated coagulation analyzer (Instrumentation Laboratory, Bedford, MA) using the SynthASil kit (Instrumentation Laboratory, Bedford, MA). Results were the average of three replicates for each type of bead. The aPTT activity of the heparin used in this study (at a concentration of 0.1 mg/mL) was 107 ± 3.0 s (standard deviation).

Surface Morphology Characterization. Field emission-scanning electron microscopy (FE-SEM) was performed to study the surface morphology of fibers with a JEOL JSM-6335 FE-SEM (Tachikawa, Tokyo, Japan) equipped with a secondary electron detector at an accelerating voltage of 10 kV and a working distance of 15 mm. Prior to performing the FE-SEM analysis, fibers were coated with gold by sputtering to form a conductive layer.

XPS. XPS experiments were performed in an ultrahigh vacuum chamber using a hemispherical electron energy analyzer (HA100, VSW, Ltd., U.K.) and a monochromatized Al X-ray source. The spectra were collected at a takeoff angle of 45°. Survey spectra were acquired with a pass energy of 117.4 eV. The binding energy scale was calibrated using the aliphatic component of the C 1s peak as 285.0 eV.

RESULTS AND DISCUSSION

Physical Property Characterization of ACBs with and without Coatings. The ACBs used in this study were prepared by the pyrolysis spherical resin.[4] The size distribution of the ACBs is shown in Figure 1A. The ACBs have and an average diameter of 520 ± 102 μm (standard deviation). The uncoated ACBs have a rough and porous surface, and cross-sectional images show matrices connected by nanoparticles (Figure 1B). The high porosity of both the surface and cross-section suggest the potential for a high adsorption rate.

In this study, we hypothesized that ACBs having a porous coating would adsorb DOX with minimal activation of the coagulation cascade, if the coating did not change the pore size significantly. DOX has a molecular dimension of 0.79 × 1.45 nm, as measured by ChemDraw 3D (Figure 1C). The pore size, distribution, surface area, and total pore volume of uncoated and coated ACBs were listed in Table 1, determined by the Brunauer–Emmett–Teller (BET) isotherm. As seen, the most frequent pore size for all types of beads is large enough (>1.6

Table 2. Heparin Content on the Surface of Coated ACBs as Analyzed by Carbazole and EDX

coated batch	milligrams of heparin per gram of beads by carbazole	percentage of heparin on the bead surface by EDX (%)
1	1.9 ± 0.2	7.0 ± 0.2
2	0.34 ± 0.03	1.2 ± 0.1
PMMA only	0	0

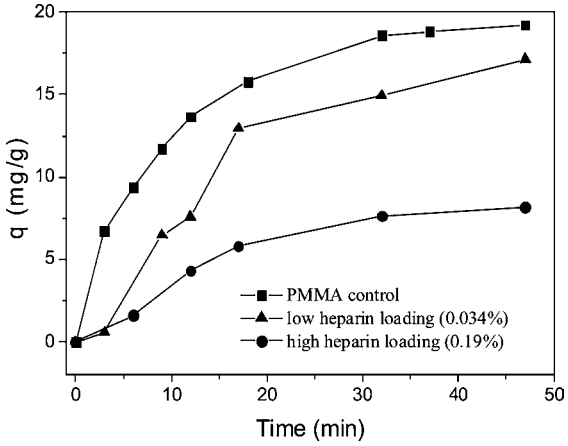

Figure 2. Kinetic curves for adsorption of DOX on beads with different coatings (adsorption performed in water; initial concentration of 0.6 mg/mL).

dx.doi.org/10.1021/la3000137 | *Langmuir* 2012, 28, 4396–4403

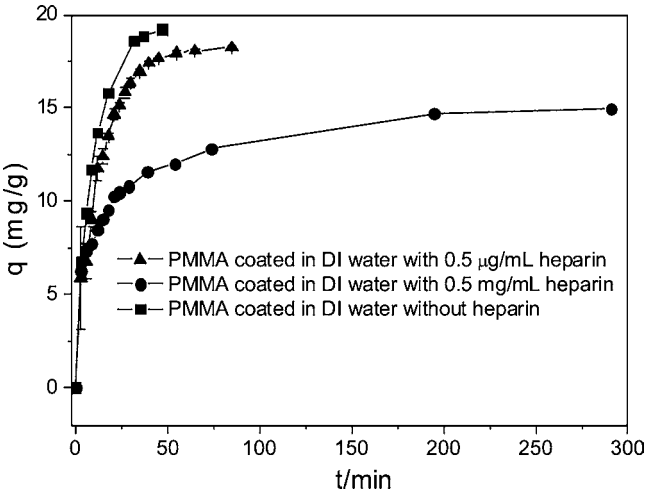

Figure 3. Heparin concentration effects on adsorption kinetics (initial concentration of DOX of 0.6 mg/mL).

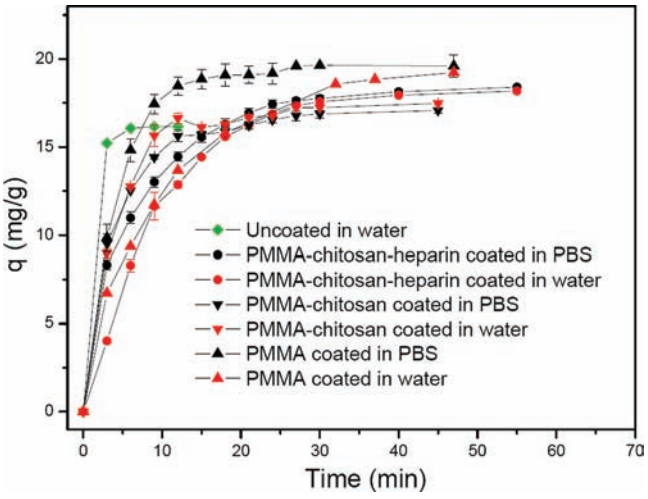

Figure 4. DOX adsorption kinetics for multicomponent-coated beads (initial concentration of DOX of 0.6 mg/mL).

Table 3. Effects of Coating and Solvent Types on the Adsorption Rate and Adsorption Capacity

type of solvents		type of coatings: uncoated beads	PMMA-coated beads	PMMA–chitosan-coated beads	PMMA–chitosan–heparin-coated beads
in PBS	time to reach equilibrium (min)	N/A	18	30	30
	equilibrium capacity (mg/g)	N/A	19.6	17.1	18.2
in water	time to reach equilibrium (min)	6	47	30	30
	equilibrium capacity (mg/g)	16.1	19.1	17.5	18.1

nm) to adsorb DOX molecules. The PMMA surface area did not change after coating and, following weight adjustment, compared to uncoated beads (average of 2325 m^2/g); however, it decreased significantly after PMMA–chitosan and PMMA–chitosan–heparin coating, following weight adjustment (average of 2040 and 1462 m^2/g, respectively), and the total pore volume also decreased accordingly, which could impact the adsorption capacity.

Adsorption of DOX on One-Step Coated ACBs. Our initial attempts to coat the PMMA/heparin blend layer on the ACB surface was inspired on the basis of our previous work,[10] and a combination of two solvents, water and acetone, were selected to dissolve both PMMA and heparin sodium at certain ratios without precipitation. The surface distribution of heparin on coated beads was acquired by scanning electron microscopy–energy-dispersive X-ray (SEM–EDX); however, the loading of heparin on a unit mass of beads was obtained other ways. First, heparin coated on the ACBs was extracted with water overnight, and then, the amount of heparin in the supernatant was determined in triplicate by the carbazole assay.[14] As shown in Table 2, batch 1 had a much higher heparin loading compared to batch 2. This high heparin loading was also confirmed in triplicate by SEM–EDX analysis (converting the obtained sulfo content to heparin content).

The adsorption kinetics curves for one-step blend coating are shown in Figure 2. Surprisingly, in comparison to PMMA-only-coated ACBs, at higher loadings of heparin on ACBs (batch 1; 0.19%), much lower adsorption rate (0.25 mg g^{-1} min^{-1}) and equilibrium adsorption capacity (8.2 mg g^{-1}) were observed. These reductions were also found in lower heparin loading (batch 2; 0.034%) with less significance. The coating of heparin may have an adverse effect on the pore size and surface area of ACBs; however, from our previous work,[10] it does not have such a significant effect on the adsorption of the drug. Considering the slow release of blend-coated heparin in aqueous solution (PMMA does not release in aqueous solution), the free heparin might have some interaction with DOX in the adsorption solution. Control experiments were designed and performed to address this issue. If batch 1 releases all of the heparin content in 3 mL adsorption solution, the concentration of heparin will be ~0.07 mg mL^{-1}; therefore, two control adsorption experiments were tested at heparin concentrations of 0.5 μg mL^{-1} and 0.5 mg mL^{-1} in water. The adsorption kinetics curves obtained are shown in Figure 3.

Initially, the adsorption rate for three conditions was similar, but the equilibrium adsorption capacity was totally different. With 0.5 mg mL^{-1} heparin in solution, the equilibrium adsorption capacity is around 15 mg g^{-1}, and it took a much longer time to reach equilibrium compared to both solution with 0.5 μg mL^{-1} heparin and without heparin. A lower heparin content had little effect on the equilibrium adsorption capacity, 18.2 versus 19.2 mg g^{-1} (without heparin).

It has been reported that one molecule of heparin can potentially complex with up to 16 molecules of DOX in an electrostatic interaction, and such a complex reduces the cytotoxicity of DOX.[15] The effect of the heparin concentration on free DOX in aqueous solution was also reported.[16] On the basis of an average molecular weight of heparin (12 000 Da), the maximum molecular weight of the heparin–DOX complex can be calculated to be 20 696 Da. Such a large macromolecular complex would undoubtedly reduce the adsorption rate and the adsorption capacity for one-step hybrid-coated ACBs.

Covalent attachment, instead of blending of heparin, on the PMMA coating is essential to reduce or eliminate the release of free heparin from the coating, improving adsorption efficiency. Unfortunately, PMMA has no available functional groups that can react directly with heparin. Chitosan, an established biocompatible matrix,[17] was coated as a second layer over

dx.doi.org/10.1021/la3000137 | Langmuir 2012, 28, 4396–4403

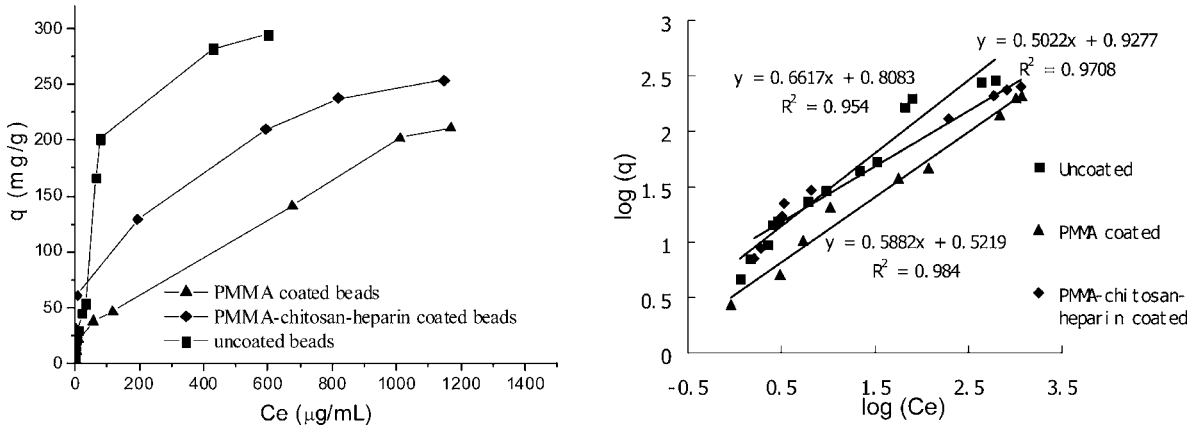

Figure 5. Adsorption isotherm (left) and linear fitting (right) on beads with different coatings in water (~10 mg in 2 mL of solution for all types of beads; equilibrium time of 12 h).

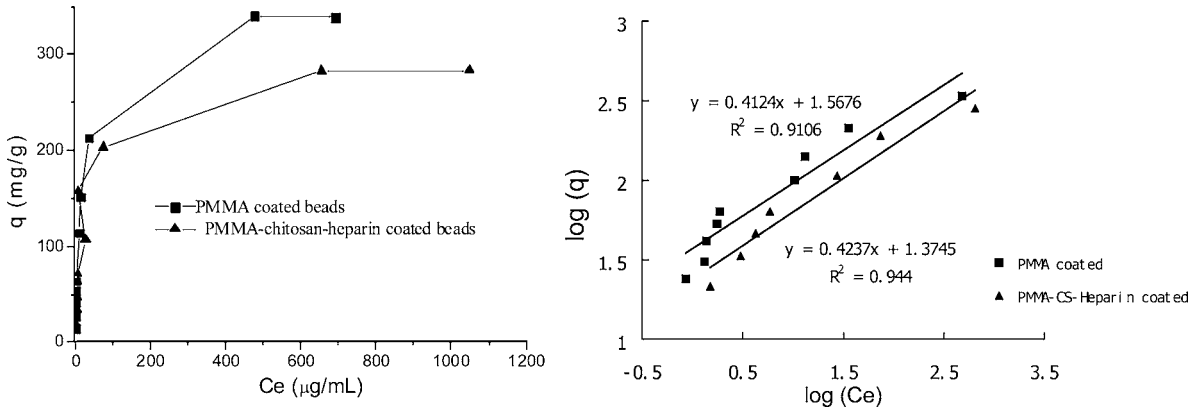

Figure 6. Adsorption isotherm (left) and linear fitting (right) on beads with different coatings in PBS (~10 mg in 2 mL of solution for all types of beads; equilibrium time of 12 h).

Table 4. Freundilich Isotherm Model Constants and Correlation Coefficients for Adsorption of DOX on Beads with and without Coating at 25 °C in Water

beads	K_F	n	R^2
uncoated	6.4	1.5	0.95
PMMA coated	3.3	1.7	0.98
PMMA−chitosan−heparin coated	8.5	2	0.97

Table 5. Freundilich Isotherm Model Constants and Correlation Coefficients for Adsorption of DOX on Beads with and without Coating at 25 °C in PBS

beads	K_F	n	R^2
PMMA coated	37	2.4	0.91
PMMA−chitosan−heparin coated	24	2.4	0.94

PMMA, because its available amino groups could then be reacted with heparin.

Adsorption Kinetics of Multilayer-Coated ACBs and Solvent Effects. PBS solution was used to measure adsorption of DOX to mimic the pH conditions in human blood.[18] PBS was also expected to reduce the electrostatic interaction between DOX and free heparin.

DOX adsorption was next measured in both water and PBS for all three types of coatings and in water only for the uncoated beads (Figure 4). The adsorption capacity has been adjusted according to the weight fraction of carbon beads. All beads with or without coating showed an initial fast adsorption and then equilibrium. The time to reach equilibrium and adsorption capacities at equilibrium are listed in Table 3.

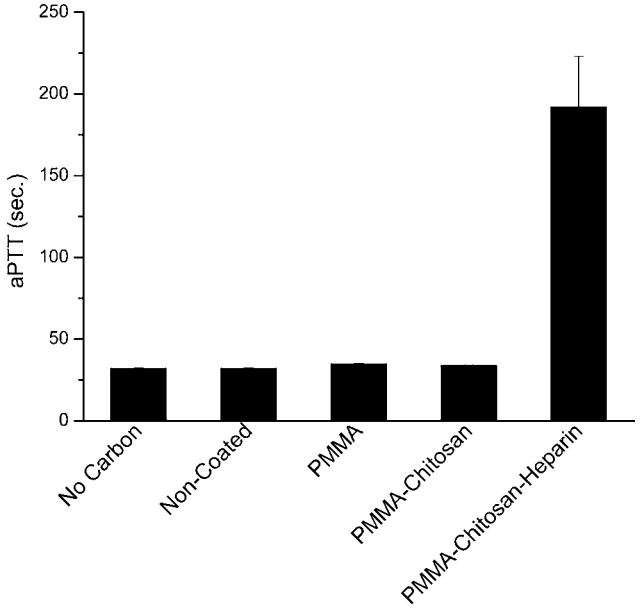

Figure 7. aPTT results for four different types of beads and a control without beads.

dx.doi.org/10.1021/la3000137 | Langmuir 2012, 28, 4396−4403

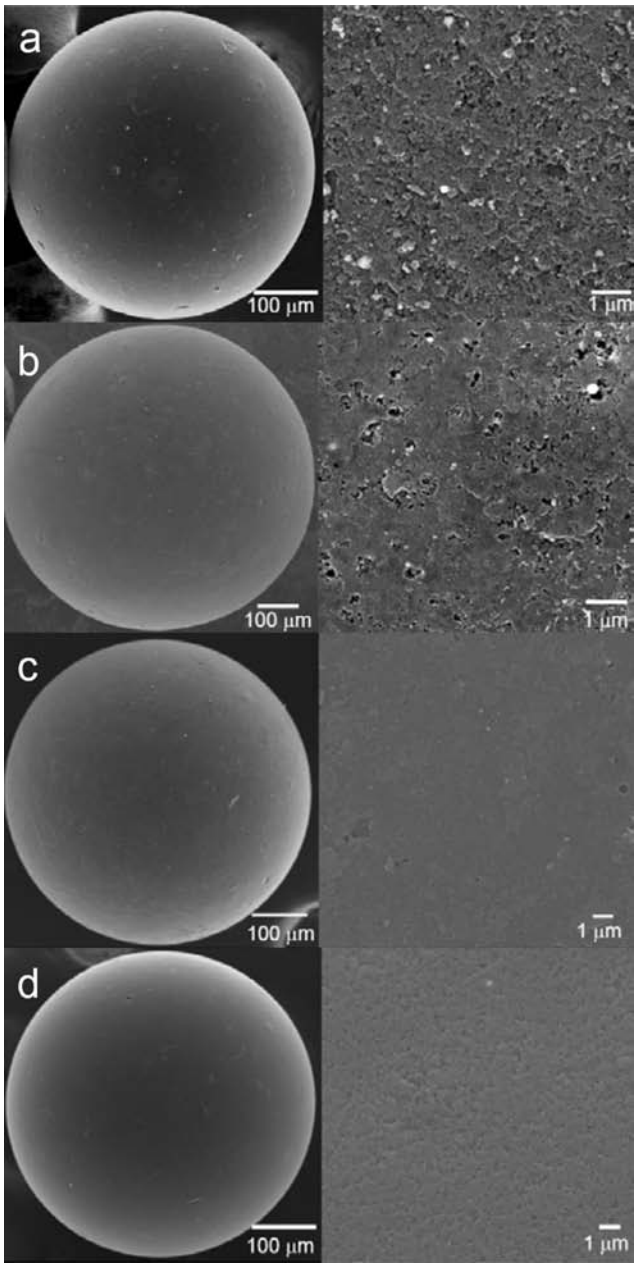

Figure 8. FE-SEM images of (a) uncoated beads, (b) PMMA-coated beads, (c) PMMA–chitosan-coated beads, and (d) PMMA–chitosan–heparin-coated beads (left panel, low magnification; right panel, high magnification).

The uncoated beads reached equilibrium most quickly in water compared to all three types of coatings; however, its equilibrium adsorption capacity was lowest. This can be explained because it is still too far away to reach saturation on uncoated beads and a lower fraction of total available adsorption sites are used compared to coated beads. PMMA–chitosan-coated and PMMA–chitosan–heparin-coated beads show similar adsorption behavior both in water and in PBS, and it took almost the same amount of time for both to reach equilibrium both in water and in PBS. The adsorption capacity at equilibrium for PMMA–chitosan–heparin-coated beads was slightly higher than that of PMMA–chitosan-coated beads, which might be attributed to the formation of the heparin–DOX complex on the surface of PMMA–chitosan–heparin-coated beads. In terms of PMMA-coated beads, the types of solvent used do have a significant effect on the adsorption rate but not on the equilibrium adsorption capacity. As we can see, these beads quickly reach equilibrium in PBS (18 min); however, they took 47 min to reach equilibrium in water. Because PMMA-coated beads have a hydrophobic surface, which might repel a hydrophilic drug, DOX may be prevented from quickly passing through the coating and reaching the adsorption sites deep within the beads. A negatively charged phosphate ion may bind 2–3 DOX hydrochloride molecules and allow for the hydrophilic portion of the drug to stay together inside and the hydrophobic portion of drug to stay outside. Thus, DOX would quickly pass through the hydrophobic coating layer, reach the adsorption sites of beads, and be adsorbed.

Adsorption Isotherm of DOX on Multilayer-Coated ACBs. The adsorption isotherm studies the relationship between the equilibrium adsorption capacity and equilibrium concentration at the same temperature. Both water and PBS were used to obtain the maximum equilibrium adsorption capacity, up to 4 mg/mL DOX. However, it was found that, at a very high DOX concentration in PBS, uncoated beads promoted the precipitation of DOX and resulted in an incorrect concentration of DOX in the supernatant. Therefore, no adsorption isotherm data for DOX in PBS are presented in the current study. Two models are typically used for studies of adsorption, the Langmuir isotherm and the Freundlich isotherm. The Langmuir isotherm is valid for monolayer adsorption on a surface with a finite number of identical sites; therefore, it is not suitable for the current study because the R^2 values are less than 90%. The Freundlich isotherm may be better to describe the current adsorption based on the heterogeneous surface of ACBs having different affinities. Its equation is as follows:[19]

$$\log q = \log K_F + (1/n)\log C_e \quad (1)$$

where q is the amount of DOX (mg) adsorbed per unit mass of the beads (g), C_e is the equilibrium concentration (μg/mL), and K_F and n are Freundlich constants related to the adsorption capacity at an equilibrium concentration of 1 μg/mL and the adsorption intensity of the adsorbent, respectively.

The fitted curves are shown in Figures 5 and 6, and the Freundlich constants and R^2 are listed in Tables 4 and 5 for water and PBS, respectively. It was found that both PMMA-coated and PMMA–chitosan–heparin-coated beads have significantly higher K_F and n values in PBS compared to those in water. Although the K_F value in PBS for PMMA-coated beads was much higher than that of PMMA–chitosan–heparin-coated beads because of a great difference in surface area, in water, the opposite effects on the K_F value were observed because of a higher hydrophobicity of PMMA coating. These observations confirmed the effects of hydrophobicity of coating and solvent types on adsorption capacity.

Blood Compatibility of ACBs with Different Coatings. aPTT, an indication of blood compatibility, was performed to measure anticoagulant activity of PMMA–chitosan–heparin-coated beads as well as other coated beads in human plasma (Figure 7). It was found that both PMMA- and PMMA–chitosan-coated beads showed a similar aPTT value to uncoated beads (32–35 s); however, PMMA–chitosan–heparin-coated beads showed a significantly higher aPTT value (192 ± 31 s) than other coated beads, which is almost double control heparin at 0.1 mg/mL and further confirmed

dx.doi.org/10.1021/la3000137 | Langmuir 2012, 28, 4396–4403

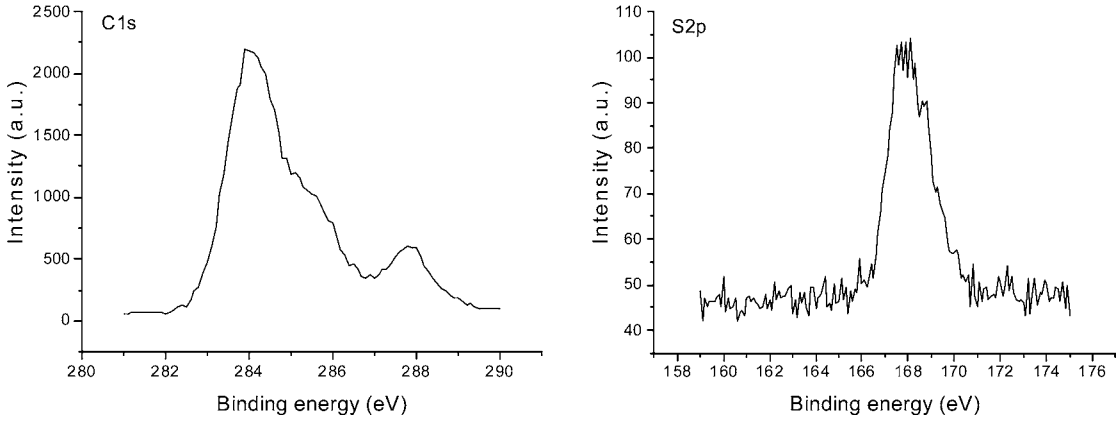

Figure 9. XPS on the PMMA−chitosan−heparin-coated beads (left panel, C 1s signal; right panel, S 2p signal).

that the covalently bound heparin on the surface of PMMA−chitosan−heparin-coated beads did not lose anticoagulation activity.

Surface Morphologies of ACBs with Different Coatings. The surface morphologies of beads with and without coating(s) were obtained by FE-SEM (Figure 8). The surface of uncoated beads has a rough and highly porous structure, with micrometer and sub-micrometer pore sizes. The internal bead structure is composed by aggregation of sub-micrometer particles seen in a cross-section of a bead (right image of Figure 1). The surface showed more smoothness than that of uncoated beads, with a large amount of available sub-micrometer-sized pores on the bead surface after coating with PMMA. PMMA−chitosan-coated beads were much smoother than either uncoated or PMMA-coated beads. PMMA−chitosan−heparin-coated beads have a relatively coarse surface compared to PMMA−chitosan-coated beads and showed a large number of available nanosized pores for adsorption of DOX. Surface elemental analysis by XPS (Figure 9) showed a signal from sulfo and ester groups (carbon signal), confirming the presence of the immobilized heparin on the PMMA−chitosan layer.

CONCLUSION

PMMA- and PMMA−chitosan−heparin-coated ACBs were prepared to improve biocompatibility and blood compatibility of these supports. One-step hybrid coating of PMMA−heparin was also performed in an acetone−water co-solvent. Increasing heparin loading on the PMMA−heparin-coated beads significantly decreased the adsorption rate and equilibrium adsorption capacity. A three-layered coating consisting of PMMA, chitosan, and covalently conjugated heparin was used to reduce the release of heparin from the coating. The adsorption kinetics indicated that solvents (water and PBS) had little effect on the adsorption rate and equilibrium adsorption capacity for both PMMA−chitosan- and PMMA−chitosan−heparin-coated beads but had a significant effect on the adsorption rate for PMMA-coated beads. The Freundlich model was used to study the adsorption isotherm and indicated the significant solvent effects on the maximum adsorption capacity for both PMMA- and PMMA−chitosan−heparin-coated beads.

A great concern of physicians using systematic drug removal systems is the sight of carbon debris leaving the filter during the procedure because these carbon fragments can lodge in small arterioles and capillaries of the lung and mimic a pulmonary embolism. Filters previously used in clinical trials exhibited low first-pass adsorption capability, produced carbon debris, and activated the blood-clotting cascade. The current adsorption system should alleviate these problems and might find potential applications in the removal of high-dose regional chemotherapy drugs while maintaining high efficiency, biocompatibility, and blood compatibility.

AUTHOR INFORMATION

Corresponding Author

*E-mail: linhar@rpi.edu.

Notes

The authors declare no competing financial interest.

ACKNOWLEDGMENTS

The authors thank the financial support from the JNC Corporation and the National Institutes of Health (NIH) in the form of Grant 1R41CA153973-01 entitled “Enabling High Dose Regional Chemotherapy while Minimizing Systemic Toxicity”.

REFERENCES

(1) Eckman, W. W.; Patlak, C. S.; Fenstermacher, J. D. Critical evaluation of principles governing advantages of intra-arterial infusions. *J. Pharmacokinet. Biopharm.* **1974**, *2* (3), 257−285.

(2) Vermorken, J. B. The role of chemotherapy in squamous-cell carcinoma of the uterine cervix—A review. *Int. J. Gynecol. Cancer* **1993**, *3* (3), 129−142.

(3) Kusunoki, N.; Ku, Y.; Tominaga, M.; Iwasaki, T.; Fukumoto, T.; Muramatsu, S.; Sugimoto, T.; Tsuchida, S.; Takamatsu, M.; Suzuki, Y.; Kuroda, Y. Effect of sodium thiosulfate on cisplatin removal with complete hepatic venous isolation and extracorporeal charcoal hemoperfusion: A pharmacokinetic evaluation. *Ann. Surg. Oncol.* **2001**, *8* (5), 449−457.

(4) Tominaga, M.; Ku, Y.; Iwasaki, T.; Suzuki, Y.; Kuroda, Y.; Saitoh, Y. Pharmacological evaluation of portal venous isolation and charcoal haemoperfusion for high-dose intra-arterial chemotherapy of the pancreas. *Br. J. Surg.* **1997**, *84* (8), 1072−1076.

(5) Jones, A.; Alexander, H. R. Development of isolated hepatic perfusion for patients who have unresectable hepatic malignancies. *Surg. Oncol. Clin. N. Am.* **2008**, *17* (4), 857−876.

(6) Maruo, T.; Motoyama, S.; Hamana, S.; Yoshida, S.; Ohara, N.; Yamasaki, M.; Ku, Y. Percutaneous pelvic perfusion with extracorporeal chemofiltration for advanced uterine cervical carcinoma. *Surg. Oncol. Clin. N. Am.* **2008**, *17* (4), 843−856.

(7) Carvalho, C.; Santos, R. X.; Cardoso, S.; Correia, S.; Oliveira, P. J.; Santos, M. S.; Moreira, P. I. Doxorubicin: The good, the bad and the ugly effect. *Curr. Med. Chem.* **2009**, *16* (25), 3267−3285.

(8) Samuel, M.; Chow, P. K. H.; Shih-Yen, E. C.; Machin, D.; Soo, K. C. Neoadjuvant and adjuvant therapy for surgical resection of hepatocellular carcinoma. *Cochrane Database Syst. Rev.* **2009**, No. 1, No. CD001199.
(9) Park, T. J.; Govindaiah, P.; Hwang, T.; Kim, E.; Choi, S. W.; Kim, J. H. Biocompatible charcoal composites prepared by ionic liquids for drug detoxification. *Macromol. Res.* **2011**, *19* (7), 734−738.
(10) Park, T. J.; Lee, S. H.; Simmons, T. J.; Martin, J. G.; Mousa, S. A.; Snezhkova, E. A.; Sarnatskaya, V. V.; Nikolaev, V. G.; Linhardt, R. J. Heparin−cellulose−charcoal composites for drug detoxification prepared using room temperature ionic liquids. *Chem. Commun.* **2008**, *40*, 5022−5024.
(11) Jager, M.; Wilke, A. Comprehensive biocompatibility testing of a new PMMA−HA bone cement versus conventional PMMA cement in vitro. *J. Biomater. Sci., Polym. Ed.* **2003**, *14* (11), 1283−1298.
(12) Lim, C. K.; Yaacob, N. S.; Ismail, Z.; Halim, A. S. In vitro biocompatibility of chitosan porous skin regenerating templates (PSRTs) using primary human skin keratinocytes. *Toxicol. in Vitro* **2010**, *24* (3), 721−727.
(13) Wissink, M. J. B.; Beernink, R.; Pieper, J. S.; Poot, A. A.; Engbers, G. H. M.; Beugeling, T.; van Aken, W. G.; Feijen, J. Immobilization of heparin to EDC/NHS-crosslinked collagen. Characterization and in vitro evaluation. *Biomaterials* **2001**, *22* (2), 151−163.
(14) Han, J. Y.; Zhang, F. M.; Xie, J.; Linhardt, R. J.; Hiebert, L. M. Changes in cultured endothelial cell glycosaminoglycans under hyperglycemic conditions and the effect of insulin and heparin. *Cardiovasc. Diabetol.* **2009**, *8*, 46−58.
(15) Mizuno, Y.; Hara, T.; Tachibana, S.; Uragoh, K.; Akazawa, K.; Ueda, K. Doxorubicin−heparin complex—Reduction of cardiotoxicity of doxorubicin. *J. Cancer Res. Clin. Oncol.* **1995**, *121* (8), 469−473.
(16) Kummerle, A.; Krueger, T.; Dusmet, M.; Vallet, C.; Pan, Y.; Ris, H. B.; Decosterd, L. A. A validated assay for measuring doxorubicin in biological fluids and tissues in an isolated lung perfusion model: Matrix effect and heparin interference strongly influence doxorubicin measurements. *J. Pharm. Biomed. Anal.* **2003**, *33* (3), 475−494.
(17) VandeVord, P. J.; Matthew, H. W. T.; DeSilva, S. P.; Mayton, L.; Wu, B.; Wooley, P. H. Evaluation of the biocompatibility of a chitosan scaffold in mice. *J. Biomed. Mater. Res.* **2002**, *59* (3), 585−590.
(18) Waugh, A.; Grant, A. *Anatomy and Physiology in Health and Illness*, 10th ed.; Churchill Livingstone Elsevier: Edinburgh, U.K., 2007; p 22.
(19) Chen, Z.; Pierre, D.; He, H.; Tan, S. H.; Chuong, P. H.; Hong, H.; Huang, J. L. Adsorption behavior of epirubicin hydrochloride on carboxylated carbon nanotubes. *Int. J. Pharm.* **2011**, *405* (1−2), 153−161.